

**This is the accepted manuscript (postprint) of the following article:**

E. Salahinejad, R. Amini, M. Marasi, M.J. Hadianfard, *The effect of sintering time on the densification and mechanical properties of a mechanically alloyed Cr–Mn–N stainless steel*, Materials and Design 31 (2010) 527–532.

<http://dx.doi.org/10.1016/j.matdes.2009.07.024>

# **The effect of sintering time on the densification and mechanical properties of a mechanically alloyed Cr–Mn–N stainless steel**

Erfan Salahinejad\*, Rasool Amini, Mehdi Marasi, Mohammad Jafar Hadianfard

Department of Materials Science and Engineering, School of Engineering, Shiraz University, Zand Blvd.

7134851154, Shiraz, Iran

## **Abstract**

Sintering is an essential stage in powder metallurgy, which affects the final microstructure and performance of the part. This study is concerned with the sintering and mechanical behaviors of Fe–18Cr–8Mn–0.9N stainless steel prepared from mechanically alloyed amorphous/nanocrystalline powders. The contribution of sintering time to the densification at 1100 °C is considered and a sluggish densification is found for the alloy. Furthermore, the correlation between the microstructure and mechanical properties of the fabricated porous parts is studied. It is found that the yield stress is affected by both porosity and the material's intrinsic yield strength. Nonetheless, the effect of porosity on the overall hardness typically prevails over the effect of matrix hardness. Interestingly, even after sintering at 1100 °C for up to 20 h, the nanometric structure of the material is retained.

**Keywords:** Nano materials (A); Powder metallurgy (C); Mechanical properties (E)

---

\* **Corresponding Author:** *Email address:* erfan.salahinejad@gmail.com

**This is the accepted manuscript (postprint) of the following article:**

E. Salahinejad, R. Amini, M. Marasi, M.J. Hadianfard, *The effect of sintering time on the densification and mechanical properties of a mechanically alloyed Cr–Mn–N stainless steel*, *Materials and Design* 31 (2010) 527–532.

<http://dx.doi.org/10.1016/j.matdes.2009.07.024>

## **1. Introduction**

Mechanical alloying (MA) of Fe-based powder mixtures under a nitrogen gas atmosphere is a very effective and efficient technique to synthesize nitrogen-supersaturated nanocrystalline and amorphous structures [1–5]. Although a good number of studies have been conducted on the characterization of these powders, little systematic work has been reported on their consolidation. It should be noted that the loss of the infused nitrogen is still a major challenge in sintering of these powders, particularly in conventional sintering atmospheres. On the other hand, to retain the attractive properties of these highly fine structures, it is technologically required to assess their thermal stability.

Explosive compaction [6], cold and hot isostatic pressing [7], and spark plasma sintering [8] methods have been examined to densificate Fe-based powders processed by MA. To our knowledge, few attempts have been made on the development of porous parts from these powders. Powder sintering is one of the efficient techniques employed to fabricate parts with spherical pores randomly distributed. Obviously, sintering strongly affects the final density, grain size, and mechanical properties of the part.

In this work, low-temperature sintering is employed for a high-nitrogen Fe–18Cr–8Mn powder synthesized by MA. The contribution of sintering time to the densification progress and mechanical properties is investigated.

## **2. Experimental work**

Fe–18Cr–8Mn–0.973N (wt.%) alloy powder was used as the primary material. This powder was produced by MA of 74Fe–18Cr–8Mn powder mixture under a nitrogen gas atmosphere, which had been milled for 48 h [1]. Other variables of the MA process were

**This is the accepted manuscript (postprint) of the following article:**

E. Salahinejad, R. Amini, M. Marasi, M.J. Hadianfard, *The effect of sintering time on the densification and mechanical properties of a mechanically alloyed Cr–Mn–N stainless steel*, *Materials and Design* 31 (2010) 527–532.

<http://dx.doi.org/10.1016/j.matdes.2009.07.024>

similar to those presented in our previous work [1]. The powder was characterized by X-ray diffraction (XRD) (Shimadzu Lab X-6000 with Cu K $\alpha$  radiation), scanning electron microscope (SEM, JEOL-JSM 5310), and transmission electron microscope (TEM, JEOL-JEM 2010). The quantitative analysis of the XRD data was carried out by TOPAS 3 from Bruker AXS. Using this software, the relative content of present phases was estimated by Rietveld method and the average crystallite size of the crystalline phases was determined by Double-Voigt approach. The amorphous phase amount was also determined by Rietveld analyzing the XRD pattern of a mixture of the as-milled powders and the known amount of nanocrystalline Fe powder as a standard. The powder:standard weight ratio of 75:25 was used for this purpose. Details of the calculations have been presented in Ref. [1]. The theoretical density of the powder particles was measured as 7.782 g/cm<sup>3</sup> by a pycnometer using He gas.

The powder was uniaxially cold-pressed to cylinders with diameter and length of 5 mm at a compressive pressure of 800 MPa. To prohibit oxidation during sintering and to preserve nitrogen in the structure, the compacts were encapsulated in quartz tubes under evacuated condition (10<sup>-5</sup> atm). A DIL 402C dilatometer (Netzch) was employed to quantify the dimensional changes in the material during non-isothermal sintering. Dilatometry was performed at a heating rate of 20 °C/min in argon. According to dilatometry results which are presented below, the densification process was carried out by sintering at 1100 °C for different times ranging from 5 to 30 h and then water-quenching to room temperature. The density of the sintered samples was determined by Archimedes water immersion method. In addition, the pores structure was observed by optical microscope. For metallographic studies, the specimens were mechanically polished up to #3000 emery paper and then finished with 1  $\mu$ m diamond paste, according to the standard procedure.

**This is the accepted manuscript (postprint) of the following article:**

E. Salahinejad, R. Amini, M. Marasi, M.J. Hadianfard, *The effect of sintering time on the densification and mechanical properties of a mechanically alloyed Cr–Mn–N stainless steel*, Materials and Design 31 (2010) 527–532.

<http://dx.doi.org/10.1016/j.matdes.2009.07.024>

The nitrogen content in the sintered samples was measured by LECO (Leco Corp., St. Joseph, MI) gas analyzer. The microstructure was investigated by XRD and TEM. For TEM observations, the samples were first cut into discs of 3 mm diameter, manually ground to about 35  $\mu\text{m}$  thickness, and then ion-milled at low temperatures.

The microhardness of pore-free zones and the bulk hardness of the sintered materials were measured on 10 points by applying 100 g and 31.25 Kg loads, respectively, and the average values are reported. To determine the yield strength of the samples (with a diameter of 5 mm and a height of 5 mm), uniaxial compression tests on the cylindrical samples were performed at room temperature with a crosshead speed of  $2 \times 10^{-5}$  m/s. At least three replicates were carried out for each specimen and the average value is reported.

### **3. Results and discussion**

#### *3.1. The as-milled powder*

Fig. 1 shows the SEM image of the powder particles. It is observed that the powders are composed of relatively rounded particles with dimensions ranging from 5 to 30  $\mu\text{m}$  and an average size of almost 10  $\mu\text{m}$ . The XRD profiles of the initial powder mixture (Fe–18Cr–8Mn) and the milled powder (Fe–18Cr–8Mn–0.973N) are indicated in Fig. 2. The Rietveld analysis of the XRD data of the as-milled powder depicted that the microstructure consists of 22.9 wt.% ferrite ( $\alpha$ ), 37.8 wt.% austenite ( $\gamma$ ), and 39.3 wt.% amorphous phase. The generation of the amorphous phase during MA has been considered from the points of view of the atomic size, heat of mixing, and extreme structural refinement [1]. The crystallite size of the  $\alpha$  and  $\gamma$  phases was estimated as 14 and 11 nm, respectively, obtained from the XRD

**This is the accepted manuscript (postprint) of the following article:**

E. Salahinejad, R. Amini, M. Marasi, M.J. Hadianfard, *The effect of sintering time on the densification and mechanical properties of a mechanically alloyed Cr–Mn–N stainless steel*, *Materials and Design* 31 (2010) 527–532.

<http://dx.doi.org/10.1016/j.matdes.2009.07.024>

analyses. This significant structural refinement is due to the severe plastic deformation subjected to the powder particles during MA.

Fig. 3 represents the TEM micrograph of a representative powder particle. The inserts are the corresponding selected area diffraction (SAD) patterns obtained from the bright and dark regions. The dark regions are a combination of the nanocrystalline  $\alpha$  and  $\gamma$  phases. The SAD pattern of the bright matrix represents a homogenous halo pattern attributed to the amorphous structure. No diffraction spots or sharp diffraction rings related to crystalline phases can be detectable and merely diffraction halos associated with the amorphous phase can be observed in these regions. It can be seen that the TEM observations verify the XRD results.

### 3.2. Sintering

The first step of powder densification is usually accomplished by pressing powder particles to create some initial contacts among them. This process should be accompanied by particle rearrangement and plastic compaction. In this work, in spite of applying a considerable compressive pressure up to 800 MPa, a relative density of as small as 69 % was obtained. It is well known that the efficiency of compaction is heavily dependent on the morphology and hardness of powder particles. The irregular morphology and high hardness of powders contribute to low green densities. In fact, poor packing behavior of powders with irregular morphologies causes a broad pore size distribution that can inhibit sintering progress. However, according to Fig. 1, the present powder particles were near-spherical in shape. Therefore, the relatively low green density is attributed to the severe plastic deformation subjected to the particles during milling, which has promoted a high level of

**This is the accepted manuscript (postprint) of the following article:**

E. Salahinejad, R. Amini, M. Marasi, M.J. Hadianfard, *The effect of sintering time on the densification and mechanical properties of a mechanically alloyed Cr–Mn–N stainless steel*, *Materials and Design* 31 (2010) 527–532.

<http://dx.doi.org/10.1016/j.matdes.2009.07.024>

strain hardening. This suppresses more plastic deformation during the cold compaction step, leading to the relatively ineffective compactability.

Fig. 4 reveals the variation in the sintering shrinkage with temperature, obtained from dilatometry. As it is seen, a dramatic drop in the shrinkage occurs at 1223 to 1360\_K. Then, the slope once again falls substantially. Based on this observed trend, the temperature of 1373 K (1100 °C) was selected for sintering and the contribution of sintering time is considered below. Note that differential scanning calorimetry results on this alloy showed that the onset crystallization temperature of the amorphous phase is nearly 580 °C [1].

The relative density of the samples sintered at 1100 °C is listed in Table 1 for the various times, showing relative densities ranging between 79 and 87.3 %. Optical micrographs taken from the specimens sintered for the different times are given in Fig. 5. The microstructures illustrate a progression from irregular to spherical pores accompanied with a tendency for pores to be isolated in their distribution by increasing the sintering time. Austenitic stainless steels are found to undergo sintering by lattice (volume) diffusion in the intermediate stage and by a combination of grain boundary and lattice diffusion in the final stage [10]. Since the sintering behavior of amorphous/nanocrystalline structures has been rarely studied, it is necessary to conduct more work that determines their sintering densification mechanism.

This observed sluggish densification behavior originates from the relatively low green density and also the presence of the amorphous phase. In our previous work [1], the thermal stability of the amorphous phase was assessed in a differential scanning calorimeter under a flowing argon gas atmosphere. The employment of this flowing atmosphere leads to the extraction of nitrogen atoms from the alloy, decreasing nitrogen concentration. However, in

**This is the accepted manuscript (postprint) of the following article:**

E. Salahinejad, R. Amini, M. Marasi, M.J. Hadianfard, *The effect of sintering time on the densification and mechanical properties of a mechanically alloyed Cr–Mn–N stainless steel*, *Materials and Design* 31 (2010) 527–532.

<http://dx.doi.org/10.1016/j.matdes.2009.07.024>

this work the application of the encapsulation technique results in the insulation of the samples in a small closed volume, thereby preserving nitrogen in the structure. On the one hand, it has been shown that the thermal stability of the amorphous phase increases by increasing the nitrogen content [1]. Hence, it is expected that during the employed sintering procedure, the thermal stability of the amorphous phase is more than that obtained from the differential scanning calorimetry results. Here, the effect of the amorphous phase presence on the densification kinetics is noticeable. Since the solubility of nitrogen is limited in the crystalline structures, nitrogen atoms tend to accumulate in the amorphous phase to decrease strain energy. The introduced N atoms occupy the interstitial sites of the atomic polyhedra or clusters of the amorphous structure, contributing to an increase in the dense random packing. This decreases the atomic diffusion coefficients, retarding densification accomplished by diffusion. On the other hand, due to the high affinity of Fe, Cr, and Mn for nitrogen and also the strong attractive bonds made up between the metal-nitrogen pairs, the N atoms do not tend to be neighbors to each other. Subsequently, the N atoms are surrounded by the metallic atoms. The presence of these stiff metal-nitrogen atomic pairs decreases the atomic mobility which is required for diffusion. Also, as the amorphous phase is the continuous phase in the microstructure, there is no rapid diffusion path like grain boundary in the structure. The contribution of these factors is responsible for slow atomic diffusivities and consequently the slow densification rate.

Meanwhile, Table 1 tabulates the nitrogen content of the specimens after sintering, obtained from the LECO analysis. This depicts that the nitrogen loss during sintering is negligible (less than 0.03 wt.%). This is attributed to the small internal volume of the sealed

**This is the accepted manuscript (postprint) of the following article:**

E. Salahinejad, R. Amini, M. Marasi, M.J. Hadianfard, *The effect of sintering time on the densification and mechanical properties of a mechanically alloyed Cr–Mn–N stainless steel*, *Materials and Design* 31 (2010) 527–532.

<http://dx.doi.org/10.1016/j.matdes.2009.07.024>

quartz capsules. This suggests that the encapsulation technique is a very efficient route to preserve nitrogen during sintering of nitrogen-containing alloys.

### *3.3. Mechanical behaviors*

The microhardness at pore-free zones, the bulk hardness, and the compressive yield stress of the porous parts are summarized in Table 2. Since the bulk hardness depends not only on the material hardness but also on the residual porosities structure, the hardness values are considerably smaller than the microhardness values at pore-free zones. On account of the relatively low density of the parts, it seems that the bulk hardness and yield stress significantly correlate with the density.

The decrease of the microhardness with increasing the sintering time results from the crystallization progress of the amorphous phase and also the coarsening of the grains. On the other hand, the increase in the macrohardness is attributed to the increase of the relative density of the specimens with sintering time. Nevertheless, as tabulated in Table 2, the yield strength reaches a maximum at 290 MPa in the sample sintered for 20 h. The increase in the yield strength of the specimens sintered for 5 h to those sintered for 20 h is owing to the increase in the relative density. In other words, in this range of density, the pores effect on the yield stress prevails over the material's intrinsic yield strength effect. In contrast, the decrease in the yield strength by increasing the sintering time after 20 h (the time causing the maximum yield stress) suggests the domination of the grain size effect on the property. That is, yielding where a negligible amount of plastic deformation is imposed is governed by both porosity and the yield strength of matrix parallelly. Yoon et al. [10] have been also reported that increasing sintering time and temperature does not vary the yield strength of 316L

**This is the accepted manuscript (postprint) of the following article:**

E. Salahinejad, R. Amini, M. Marasi, M.J. Hadianfard, *The effect of sintering time on the densification and mechanical properties of a mechanically alloyed Cr–Mn–N stainless steel*, *Materials and Design* 31 (2010) 527–532.

<http://dx.doi.org/10.1016/j.matdes.2009.07.024>

stainless steels, due to the balanced effects of decrease of porosity and grain coarsening.

However, in this study the material exhibited a maximum in yield stress at 20 h increasing.

From the results of this study, it can be inferred that the macrohardness correlates with the density more than the hardness of matrix. In other words, the effect of grain size on the hardness is not significant in this study. During macro-indentation a considerable amount of plastic deformation is locally given; consequently, the role of grain size diminishes and hardness values are typically controlled by the pores effect. On the other hand, it is well known that tensile strength is typically controlled by microvoid growth and coalescence [10]. Since hardness is well proportional to tensile strength, this can justify the observed hardness behavior. Albeit, this does not mean that grain size has no effect on hardness. In the same conditions of pores structure, grain size is surely effective on the hardness variation significantly. It has been also reported that the contribution of porosity and inclusions to the tensile strength, elongation, and fracture behavior of sintered 316L stainless steels prevails over that of grain size [10–12]. It is noted that in the fracture similar to the macro-indentation, considerable amounts of plastic deformation is subjected.

Fig. 6 signifies the XRD pattern of the part sintered for 20 h, demonstrating a fully  $\gamma$  structure with a crystallite size of 90 nm. The TEM image of this sample confirms the XRD results, as presented in Fig. 7. Hence, sintering at 1100 °C for 20 h develops nanostructured austenitic stainless steels with a relative density of 86 % and almost spherical pores. The considerable mechanical properties of this sample, despite the relatively low density, are attributed to its high nitrogen concentration and nano scale structure.

It is noteworthy that despite the long sintering time, no significant grain growth in the sample sintered for 20 h has occurred. That is, the material has shown a considerable thermal

**This is the accepted manuscript (postprint) of the following article:**

E. Salahinejad, R. Amini, M. Marasi, M.J. Hadianfard, *The effect of sintering time on the densification and mechanical properties of a mechanically alloyed Cr–Mn–N stainless steel*, *Materials and Design* 31 (2010) 527–532.

<http://dx.doi.org/10.1016/j.matdes.2009.07.024>

stability related to an inherent resistance to grain growth. It is well known that the grain growth kinetics is governed by grain boundary mobility. The main factors affecting grain boundary mobility in nanostructures are grain boundary segregation, solute drag, pore drag, chemical ordering, and secondary phase (Zener) drag [3,13]. In the present study, it is recognized that the retarded grain growth can be a consequence of the segregation of nitrogen atoms to grain boundaries, the retarded crystallization of the amorphous phase existing in the as-milled powder, and the presence of pores on the grain boundaries. Since the solubility of nitrogen is limited in crystalline structures, nitrogen atoms tend to segregate toward grain boundaries to decrease strain energy. The accumulation of considerable nitrogen content at grain boundaries retards grain growth. Also, it has been shown that the stability of the amorphous phase created during MA under the nitrogen gas atmosphere is significant [1]. Thus, the crystallization of this phase is expected to be a slow transformation, which can affect the resultant grain size.

Eventually, it should be mentioned that whereas conventional sintering at higher temperatures, hot isostatic pressing, or spark plasma sintering can give rise to more densities, in some applications porous structures with adequate mechanical properties are attractive, especially in the biomaterials field. Porous materials with sufficient mechanical properties have been recognized as desired bone implants for the last decade. The porous implants provide a better fixation of implants to the bone host, via the growth of new bone tissue into the pore spaces. Furthermore, introducing pores into stainless steel parts results in a decrease in the mismatch of elastic moduli of the implant and surrounding bone, thereby improving the fixation [14]. It has been also reported that pores in lubricant conditions, such as human body act as a reservoir of fluids, decreasing the friction coefficient and material wear [15]. On the

**This is the accepted manuscript (postprint) of the following article:**

E. Salahinejad, R. Amini, M. Marasi, M.J. Hadianfard, *The effect of sintering time on the densification and mechanical properties of a mechanically alloyed Cr–Mn–N stainless steel*, *Materials and Design* 31 (2010) 527–532.

<http://dx.doi.org/10.1016/j.matdes.2009.07.024>

other hand, in this work the preservation of nitrogen in the structure is attributed to the application of the encapsulation technique. Other sintering process can not retain infused nitrogen in the structure. Details of the microstructural, mechanical, and corrosion behaviors of these porous materials will be published elsewhere.

#### **4. Conclusion**

The sintering behavior of mechanically alloyed Fe–18Cr–8Mn–0.973N powder at 1100 °C and the effect of sintering time on mechanical properties were assessed. The outcome of this study can be summarized as follows:

(1) The contribution of sintering time to the densification progress was assessed and the slow densification was observed.

(2) The nitrogen loss during sintering was found to be negligible due to the employment of the encapsulation technique.

(3) The retarded grain growth during sintering was attributed to: (i) the grain boundary segregation of nitrogen atoms, (ii) the slow crystallization of the amorphous phase, and (iii) the pores drag.

(4) Sintering at 1100 °C for 20 h developed a porous austenitic stainless steel with a relative density of 86 % and spherical pores. It is noticeable that the grain size of this sample after sintering was remained in the nano-scale range.

(5) The yield stress was found to be affected by both porosity and the material's intrinsic yield strength. However, the porosity effect on the overall hardness dominated the effect of matrix hardness.

**This is the accepted manuscript (postprint) of the following article:**

E. Salahinejad, R. Amini, M. Marasi, M.J. Hadianfard, *The effect of sintering time on the densification and mechanical properties of a mechanically alloyed Cr–Mn–N stainless steel*, *Materials and Design* 31 (2010) 527–532.

<http://dx.doi.org/10.1016/j.matdes.2009.07.024>

(6) The maximum of the yield stress was found for the specimens sintered for 20 h, due to the compromise between the material's intrinsic hardness and the pores.

## References

- [1] Amini R, Hadianfard MJ, Salahinejad E, Marasi M, Sritharan T. Microstructural phase evaluation of high-nitrogen Fe–Cr–Mn alloy powders synthesized by the mechanical alloying process. *J Mater Sci* 2009;44:136-48.
- [2] Amini R, Shokrollahi H, Salahinejad E, Hadianfard MJ, Marasi M, Sritharan T. Microstructural, thermal and magnetic properties of amorphous/nanocrystalline FeCrMnN alloys prepared by mechanical alloying and subsequent heat treatment. *J Alloys Compd* 2009;480:617-24.
- [3] Cisneros MM, Lopez HF, Mancha H, Vazquez D, Valdes E, Mendoza G, Mendez M. Development of austenitic nanostructures in high-nitrogen steel powders processed by mechanical alloying. *Metall Mater Trans A* 2002;33:2139-44.
- [4] Mendez M, Mancha H, Cisneros MM, Mendoza G, Escalante JI, Lopez HF. Structure of a Fe–Cr–Mn–Mo–N alloy processed by mechanical alloying. *Metall Mater Trans A* 2002;33:3273-8.
- [5] Cisneros MM, Lopez HF, Mancha H, Rincon E, Vazquez D, Perez MJ, Torre SDDL. Processing of nanostructured high nitrogen stainless steel by mechanical alloying. *Metall Mater Trans A* 2005;36:1309-16.
- [6] Rawers J, Govier D, Korth G. Consolidation, mechanical properties and phase stability of mechanically alloyed Fe–N powder compositions. *ISIJ Int* 1996;36:947-50.

**This is the accepted manuscript (postprint) of the following article:**

E. Salahinejad, R. Amini, M. Marasi, M.J. Hadianfard, *The effect of sintering time on the densification and mechanical properties of a mechanically alloyed Cr–Mn–N stainless steel*, *Materials and Design* 31 (2010) 527–532.

<http://dx.doi.org/10.1016/j.matdes.2009.07.024>

- [7] Munitz A, Livne Z, Rawers JC, Adams JS, Fields RJ. Effect of nitrogen on the mechanical properties and microstructure of hot isostatically pressed nanograined Fe. *Nanostruct Mater* 1999;11:159-77.
- [8] Jing L, Guang-qiang L, Bing P, Xin Z. Effect of nitrogen on structure and properties of ultra-fine austenitic stainless steel. *Proceedings of Sino-Swedish Structural Materials Symposium 2007*;310-5.
- [9] Suri P, Koseski RP, German RM. Microstructural evolution of injection molded gas- and water-atomized 316L stainless steel powder during sintering. *Mater Sci Eng A* 2005;402:341-8.
- [10] Yoon TS, Lee YH, Ahn SH, Lee JH, Lee CS. Effects of sintering conditions on the mechanical properties of metal injection molded 316L stainless steel. *ISIJ Int* 2003;43:119-26.
- [11] Lindstedt U, Karlsson B, Nyström M. Small fatigue cracks in an austenitic stainless steel. *Fatigue Fract Eng Mater Struct* 1998;21(1):85-98.
- [12] Lindstedt U, Karlsson B. Microstructure and mechanical behaviour of single pressed and vacuum sintered gas and water atomised 316L stainless steel powders. *Powder Metall* 1998;41(4):261-8.
- [13] Malow TR, Koch CC. Grain growth in nanocrystalline iron prepared by mechanical attrition. *Acta Mater* 1997;45:2177-86.
- [14] Dewidar MM, Khalil KA, Lim JK. Processing and mechanical properties of porous 316L stainless steel for biomedical applications. *Trans Nonferrous Met Soc China* 2007;17:468-73.
- [15] Gradzka-Dahlke M, Dabrowski JR, Dabrowski B. Characteristic of the porous 316 stainless steel for the friction element of prosthetic joint. *Wear* 2007;263:1023-9.

This is the accepted manuscript (postprint) of the following article:

E. Salahinejad, R. Amini, M. Marasi, M.J. Hadianfard, *The effect of sintering time on the densification and mechanical properties of a mechanically alloyed Cr–Mn–N stainless steel*, *Materials and Design* 31 (2010) 527–532.

<http://dx.doi.org/10.1016/j.matdes.2009.07.024>

**Figures:**

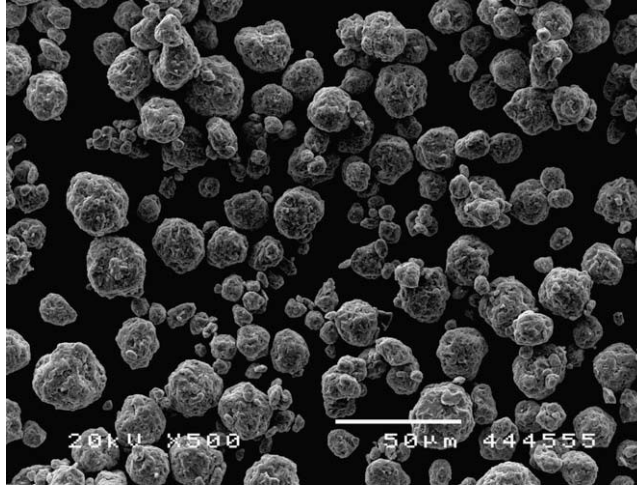


Fig. 1. SEM micrograph of the Fe–18Cr–8Mn–0.973N powder particles synthesized by MA.

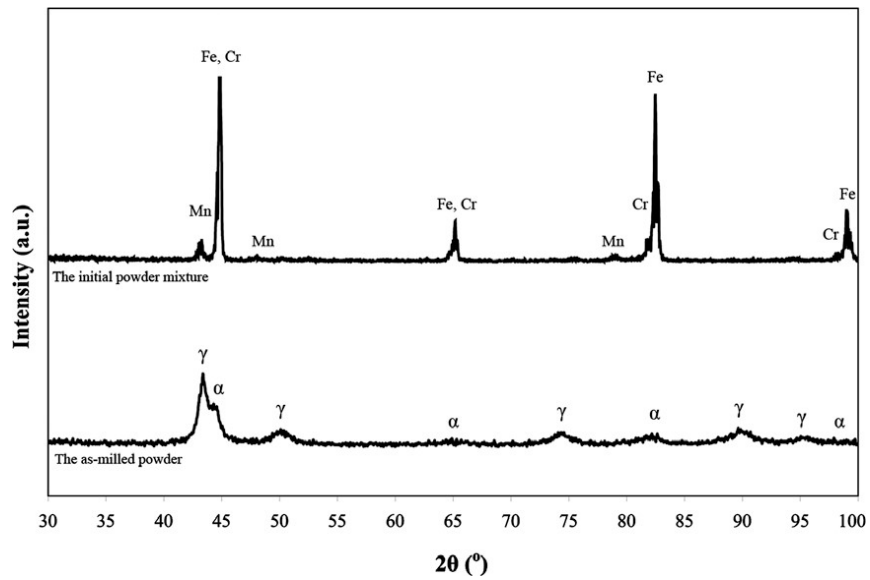


Fig. 2. XRD profile of the initial and as-milled powders.

This is the accepted manuscript (postprint) of the following article:

E. Salahinejad, R. Amini, M. Marasi, M.J. Hadianfard, *The effect of sintering time on the densification and mechanical properties of a mechanically alloyed Cr–Mn–N stainless steel*, *Materials and Design* 31 (2010) 527–532.

<http://dx.doi.org/10.1016/j.matdes.2009.07.024>

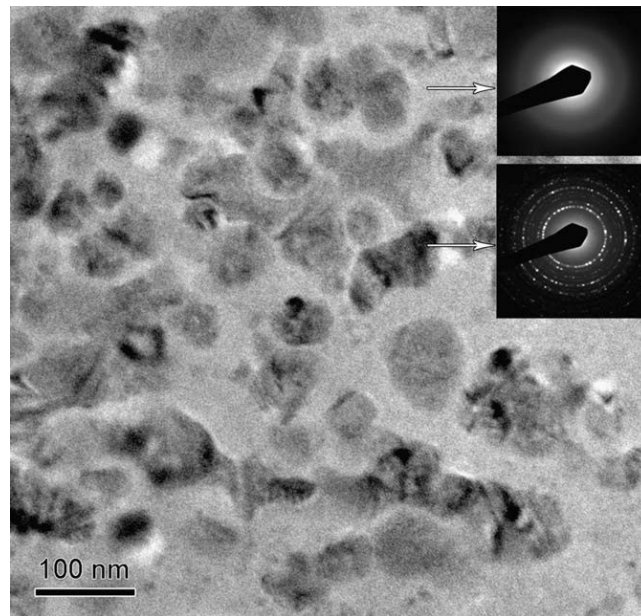


Fig. 3. TEM micrograph of the as-milled powder and the corresponding SAD patterns.

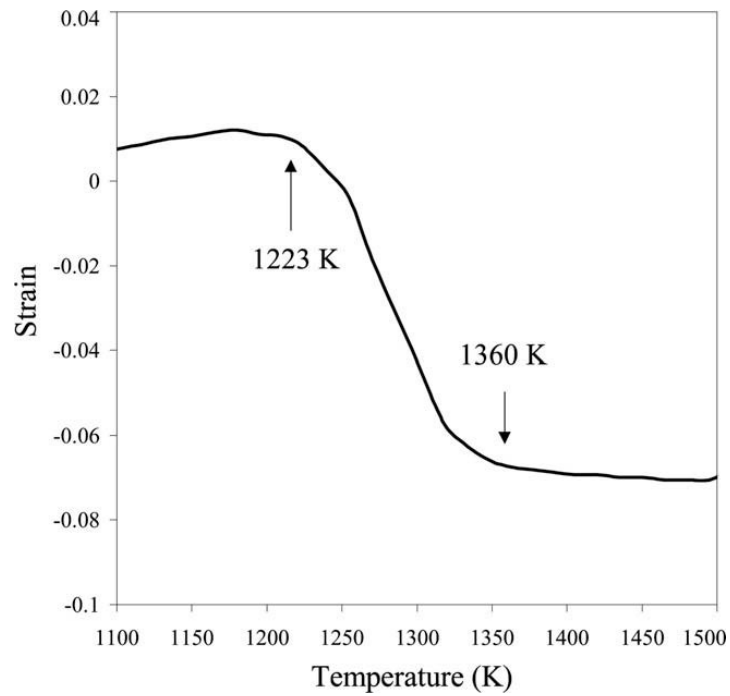


Fig. 4. Dilatometric curve of the powder.

This is the accepted manuscript (postprint) of the following article:

E. Salahinejad, R. Amini, M. Marasi, M.J. Hadianfard, *The effect of sintering time on the densification and mechanical properties of a mechanically alloyed Cr–Mn–N stainless steel*, *Materials and Design* 31 (2010) 527–532.

<http://dx.doi.org/10.1016/j.matdes.2009.07.024>

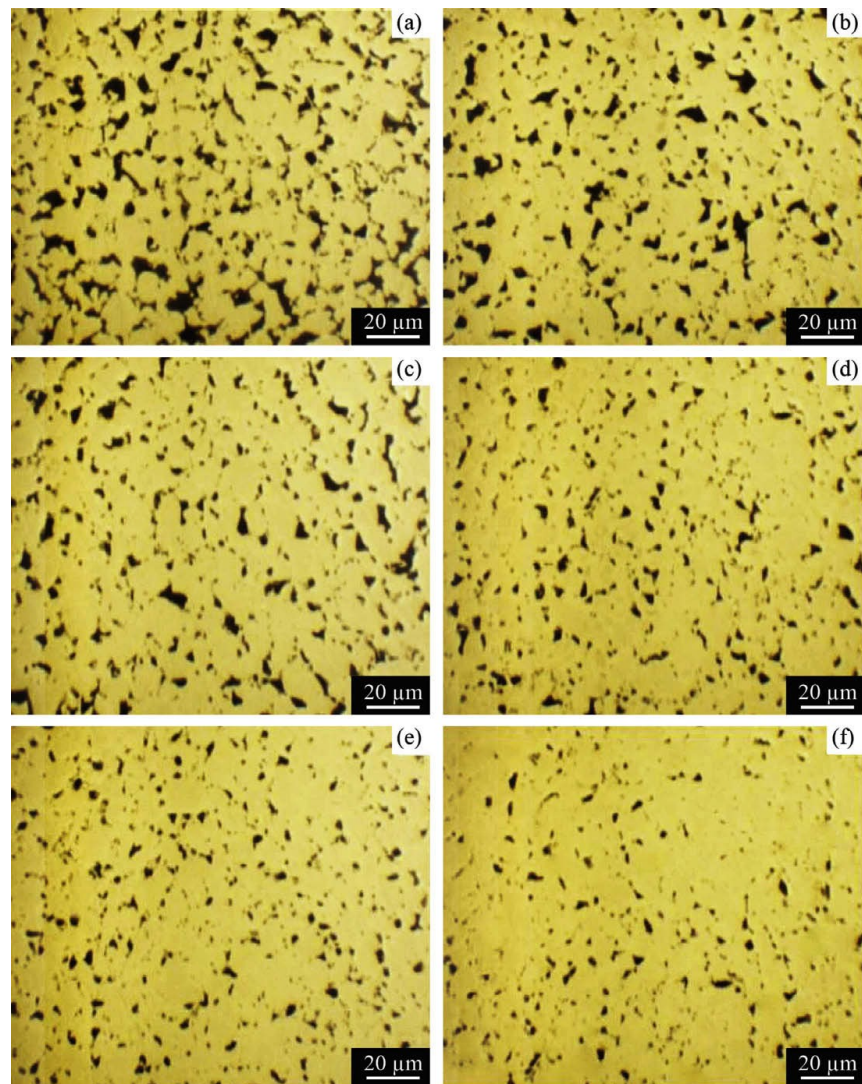


Fig. 5. Optical micrograph of the specimens sintered at 1100 °C for the various times: (a) 5 h, (b) 10 h, (c) 15 h, (d) 20 h, (e) 25 h, and (f) 30 h.

This is the accepted manuscript (postprint) of the following article:

E. Salahinejad, R. Amini, M. Marasi, M.J. Hadianfard, *The effect of sintering time on the densification and mechanical properties of a mechanically alloyed Cr–Mn–N stainless steel*, *Materials and Design* 31 (2010) 527–532.

<http://dx.doi.org/10.1016/j.matdes.2009.07.024>

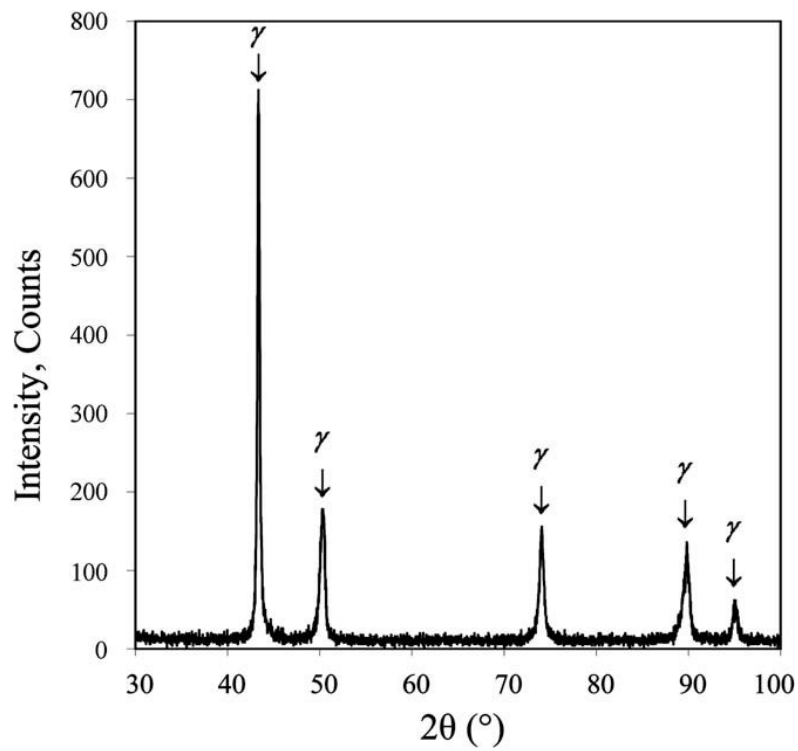


Fig. 6. XRD pattern of the sample sintered at 1100 °C for 20 h.

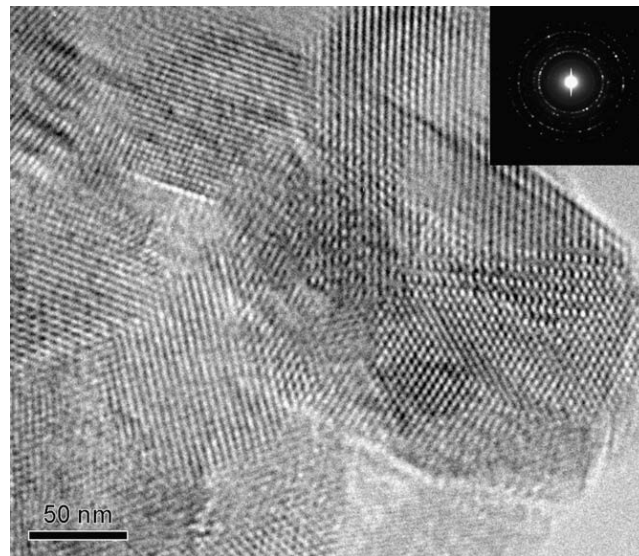


Fig. 7. TEM micrograph of the specimen sintered for 20 h.

**This is the accepted manuscript (postprint) of the following article:**

E. Salahinejad, R. Amini, M. Marasi, M.J. Hadianfard, *The effect of sintering time on the densification and mechanical properties of a mechanically alloyed Cr–Mn–N stainless steel*, *Materials and Design* 31 (2010) 527–532.

<http://dx.doi.org/10.1016/j.matdes.2009.07.024>

Table 1. The relative density and the nitrogen concentration of the samples sintered at 1100

°C for the various times

Sintering time (h)	Relative density (%)	Nitrogen content (wt.%)
5	79.0	0.959
10	81.8	0.968
15	84.5	0.952
20	86.0	0.954
25	86.9	0.948
30	87.3	0.946

Table 2. The mechanical properties of the sintered specimens

Sintering time (h)	Hardness (Hv)	Microhardness (Hv)	Yield stress (MPa)
5	95 <5>	770 <18>	190 <10>
10	105 <5>	725 <15>	220 <10>
15	125 <10>	676 <15>	245 <5>
20	140 <5>	350 <10>	290 <10>
25	145 <5>	336 <10>	285 <5>
30	160 <10>	324 <8>	270 <5>

Error value: <X> = ±X